



Recent developments in the computational study of protein structural and vibrational energy dynamics

David M. Leitner^{1,2} · Takahisa Yamato²

Received: 6 January 2020 / Accepted: 23 February 2020

© International Union for Pure and Applied Biophysics (IUPAB) and Springer-Verlag GmbH Germany, part of Springer Nature 2020

Abstract

Recent developments in the computational study of energy transport in proteins are reviewed, including advances in both methodology and applications. The concept of energy exchange network (EEN) is discussed, and a recent calculation of EENs for the allosteric protein FixL is reviewed, which illustrates how residues and protein regions involved in the allosteric transition can be identified. Recent work has examined relations between EENs and protein dynamics as well as structure. We review some of the computational studies carried out on several proteins that explore connections between energy conductivity across polar contacts in proteins and between proteins and water and equilibrium dynamics of the contacts, and we discuss some of the recent experimental work that addresses this topic.

Keywords Proteins · Energy transport · Energy exchange network · FixL · Hemoglobin

Introduction

Theoretical, computational, and experimental studies of energy transport in and between biological molecules continue to provide more detailed information about relations between protein dynamics and function (Leitner 2008; Leitner and Straub 2010; Nagy et al. 2005). Energy flow in molecules influences chemical reaction kinetics, and the interpretation of a wide range of spectroscopic experiments on proteins requires information about energy relaxation and transport. We recently reviewed the status of computational studies of energy transport in proteins (Leitner and Yamato 2018). Here, we summarize recent developments in that area and new applications. We review recent work on the computation and identification of energy exchange networks (EENs) for the allosteric protein FixL (Ota and Yamato 2019), by which residues and

regions important in allosteric transitions have been identified. We also summarize the recent efforts to relate the energy conductivity across non-bonded contacts, i.e., non-covalent contacts, to the dynamics of the contact. In this way, we relate EENs not only to the structures sampled by a protein in a functional state but also to protein dynamics.

In Section 2, we discuss recent calculations of EENs for the allosteric protein FixL (Ota and Yamato 2019). That section highlights the changes that occur in EENs along regions of the protein that play a role in allosteric transitions. The networks include energy conductivity between non-bonded contacts, which depend both on protein structure and dynamics. In Section 3, we discuss recent computational work examining relations between biomolecule structure, equilibrium structural fluctuations, and energy conductivity across hydrogen bonds. A central theme is the relation between equilibrium structural fluctuations and rates of energy transfer across contacts between amino acids, cofactors, and water. We conclude in Section 4 with discussion of some of the recent experiments that test some of the computational and theoretical work summarized in this review and comment on future directions.

✉ David M. Leitner
dml@unr.edu
✉ Takahisa Yamato
yamato@nagoya-u.jp

¹ Department of Chemistry and Chemical Physics Program, University of Nevada, Reno, NV 89557, USA

² Graduate School of Science, Division of Material Science, Nagoya University, Furo-cho, Chikusa-ku, Nagoya 464-8602, Japan

Energy exchange network (EEN) for FixL

To analyze the network of interacting amino acid residues within a thermally fluctuating protein molecule under

physiological conditions, we introduced the concept of EEN (Ishikura et al. 2015). In such an environment, the amino acid residues are tightly packed and constantly exchange heat and energy with each other. It has been demonstrated that the rate of energy transfer between each pair of interacting residues depends both on the static and dynamical properties of the native protein molecule (Buchenberg et al. 2016; Fujii et al. 2011, 2014; Kondoh et al. 2016; Leitner et al. 2015; Mizutani 2017; Yamashita et al. 2018). Also, flow of heat and energy in a protein can be characterized in terms of transport coefficients calculated by equilibrium molecular dynamics (MD) simulations based on linear response theory (Ishikura et al. 2015; Ishikura and Yamato 2006; Ota and Yamato 2019; Yamato 2010).

Since the native structure of a folded protein is highly anisotropic and inhomogeneous, it would be an oversimplification to represent the transport property of the entire molecule with just a single value of the spatially averaged transport coefficient. To quantitatively evaluate the functional significance of each individual site within a protein molecule, we calculate the local energy conductivity, rather than the overall one, for each pair of amino acid residues. This quantity is hereafter denoted as inter-residue energy conductivity, G , for which a brief note is in order. The energy conductivity might sound like an unfamiliar term. We can readily show that G is roughly proportional to the thermal conductivity, with which we are familiar, for a robust molecular system such as a folded protein. In our studies, we have been mostly focused on the non-bonded native contacts because such contacts occur after folding has made a protein functional. For a particular protein of interest, we are able to draw a map of the EEN, in which each residue is represented as a node, and a pair of nodes is connected with a segment if the pair has G greater than a chosen threshold value. The EEN map provides a simple coarse-grained representation of a particular protein state, yet every detail of atomic interactions is reflected on the map because we calculate G based on all-atom MD simulations.

From energetical point of view, native non-bonded contacts are characterized with interaction energies of intermediate strengths; they are mostly robust in the native state, while some of them can be reorganized after external stimuli such as ligand binding. We expect that transitions between different states of a protein should be associated with the changes in G , especially at the functionally important sites. Accordingly, the effect of an external stimulus on EEN is represented by the difference map of EEN, hereafter referred to as Δ EEN.

As an application, we studied the allosteric transition in an oxygen sensor protein, FixL (Ota and Yamato 2019). This protein consists of multiple domains. The oxygen sensing domain, FixLH, is bound to the heme group and connected via its coiled-coil linker to the histidine kinase (HK) domain that is active under anaerobic conditions. This HK activity is, in

turn, suppressed under aerobic conditions by O_2 binding to the heme group. It is noteworthy that the X-ray crystallography of the FixLH monomer in the deoxy- and oxy forms demonstrated that the structural change by ligand binding is very small. So the question is how such a small change leads to signaling. Recently, the full-length structure of FixL was modeled by small-angle X-ray scattering and X-ray crystallography (Wright et al. 2018). It has been widely accepted that FixL forms a dimer in solution (Fig. 1), but this exhibits no cooperativity in ligand binding. Accordingly, we conjectured that the early event immediately after ligand binding occurs primarily within the monomeric unit of FixLH. Many researchers believe that quaternary structural changes occur in the FixL dimer in the signaling processes. To study the molecular signaling mechanism of this system, we performed MD simulations of both deoxy- and oxy FixLHs, and calculated G_{deoxy} and G_{oxy} , respectively. In Fig. 2, we show the Δ EEN map between the two forms based on the analysis of $\delta G \equiv G_{\text{oxy}} - G_{\text{deoxy}}$. The average value and standard deviation of δG are denoted as $\bar{\delta}G$ and σ , respectively. Interestingly, *cluster 1* is mainly located at the dimer interface, while *cluster 2* is in the junction between the C-terminus of FixLH and the coiled-coil linker, indicating that these regions play important roles in the signaling mechanism (Fig. 1). We identified each cluster as a set of surface-exposed amino acid residues that experienced large δG by ligand binding. It is worth mentioning that *cluster 1* and 2 constitute mutually independent subgraphs in the map of Δ EEN (Fig. 2). *Cluster 1* (2) extends over loops AB, FG, and strands H β , I β (GH-loop, I β strand and C α helix). Note that publicly available data of a high-resolution structure of FixLH dimer is still missing, and we need close collaboration with structural biologists for further study.

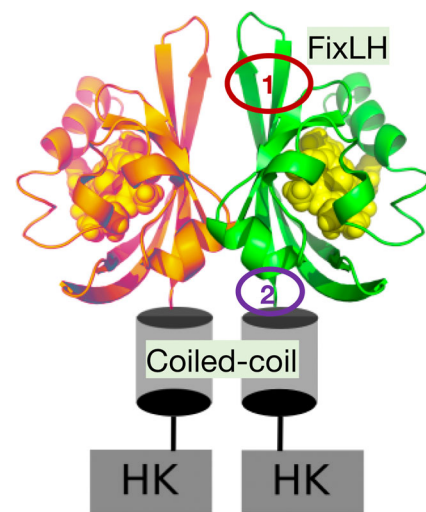
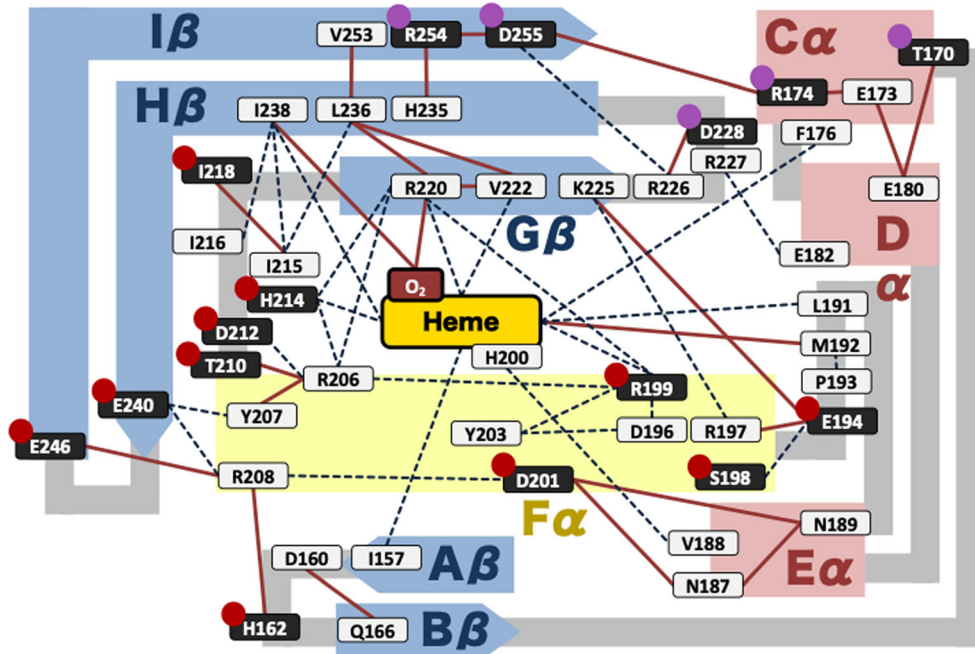


Fig. 1 Schematic view of the FixL dimer. The FixLH monomer is connected via the coiled-coil linker with the HK domain. The locations of *cluster 1* and 2 are indicated by brown and purple circles, respectively (see Fig. 2)

Fig. 2 Δ EEN map between oxy and deoxy FixLHs. Each amino acid residue is represented by a node shown as a rounded rectangle with its one letter amino acid code and sequential number. The oxygen ligand is represented as a brown rounded rectangle. Residue pairs with $\delta G \geq (<) \overline{\delta G} + (-) \sigma$ are connected by solid (broken) segments. Surface exposed residues are represented as filled rectangles. These residues are separated into two different clusters, where cluster 1 and 2 are indicated by brown and purple circles, respectively. Reprinted from (Ota and Yamato 2019), Copyright (2019), American Chemical Society.



Vibrational energy transfer and equilibrium structural fluctuations

In the previous section, we have seen how the network of local energy conductivity, or energy exchange network (EEN), depends on the functional states of a protein and can point to protein regions important in allosteric transitions. Underlying the energy conductivity, G , is not only the protein structure but also dynamics, so that the Δ EEN map identifies changes in both protein structure and dynamics that correspond to change of state. In recent work, we have been turning our attention to the specific role of structure and dynamics in mediating the values of G . In this section we summarize recent work on exploring relations between rates of energy transfer across non-bonded contacts between protein residues and between residues and water and protein dynamics, with the aim of examining how G is influenced by the dynamics of the contact. As a specific case, we discuss hydrogen bonds between residue pairs and between residues and water. Hydrogen bonds are only defined for short contact distance, so that structure clearly contributes to G . When the hydrogen bond is not intact, the energy conductivity across such a contact is very small. While energy transfer could still occur through a van der Waals contact, in this case, the rate of this process is typically one or two orders of magnitude smaller than energy transfer across a hydrogen bond (Buchenberg et al. 2016). However, when the hydrogen bond is formed, we shall see that the value of G is determined to a large extent by the dynamics of the contact.

For short-range contacts such as hydrogen bonds and van der Waals contacts, the rate of energy transfer was first observed to be related to equilibrium structural fluctuations in

the computational study of energy transport in HP36 (Buchenberg et al. 2016). That work found that energy transport predicted by all-atom non-equilibrium simulations could be modeled well by a Markov model at the length scale of amino acid residues. Energy transport predicted by a master equation reproduced the results of the all-atom simulations quite well. The study also indicated that the rate constants in the master equation were related to fluctuations in the contact distance, i.e., structural fluctuations computed by short equilibrium simulations could predict rate constants for non-equilibrium master equations simulations (Leitner et al. 2015) of energy transport in proteins and protein complexes. More specifically, the rate constant for energy transfer across a non-bonded contact was found to be proportional to the inverse of the variance in the length of the contact. To enhance signal to noise, the all-atom non-equilibrium molecular dynamics simulations of HP36 were carried out at energies corresponding to temperatures below 50 K.

We have since examined computationally the relation between the local energy conductivity between non-bonded contacts interacting by hydrogen bonds and the variance in the distance of the hydrogen bond for myoglobin at 300 K (Reid et al. 2018). We again found that, for non-bonded contacts interacting by short-range potentials, the energy transfer rate across the contact varies inversely with the variance in the contact length. A similar relation was found for the hydrogen-bonded contacts of the dimeric hemoglobin from *Scapharca Inaequivalvis*, HbI, in the unliganded state, including contacts with water molecules at the interface of the two globules (Leitner et al. 2019; Reid et al. 2020).

To illustrate the scaling between energy conductivity, proportional to the rate constant for energy transfer between two

non-bonded contacts, and the inverse of fluctuations in the contact length, we show in Fig. 3 results computed for hydrogen bonded residues of the dimeric hemoglobin from *Scapharca Inaequivalvis*, HbI, in the unliganded state. As in the earlier work on myoglobin, the comparison of equilibrium fluctuations and energy transfer rates is made for the same trajectory from a molecular simulation, using the current calculation for proteins (CURP) computational approach (Ishikura et al. 2015; Ishikura and Yamato 2006; Yamato 2010). As in earlier computational work with CURP, the energy conductivity, G , obtained from the time-correlation function of the inter-residue energy current (Ishikura et al. 2015;

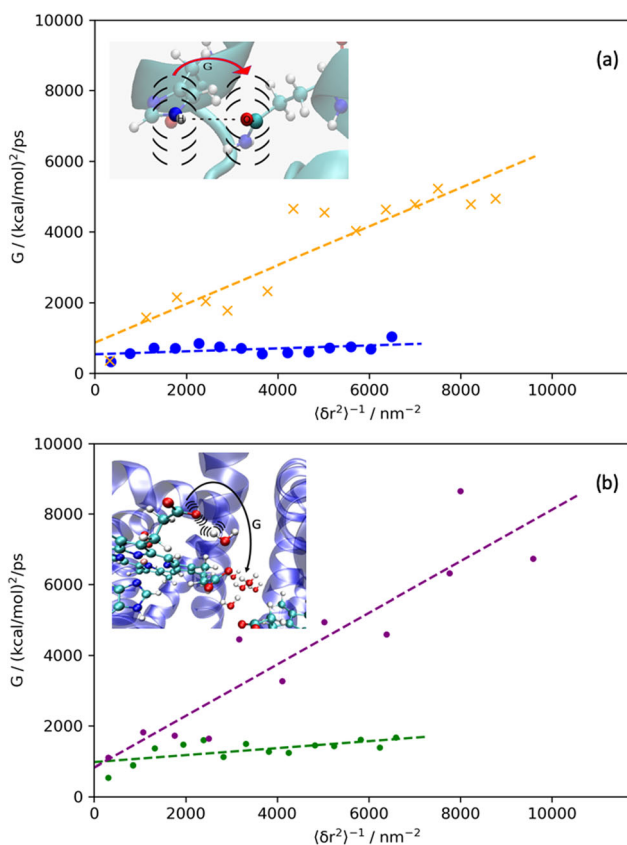


Fig. 3 (a) Energy conductivity, G , across polar contacts of deoxy-HbI as a function of the inverse of the variance, $\langle \delta r^2 \rangle^{-1}$, in the length of that contact. The data appear to fall on two lines for different sets of polar contacts. The contacts represented by the orange data points and the contacts represented by the blue data points are detailed in (Reid et al. 2020); (b) Energy conductivity, G , between the cluster of water molecules at the interface of deoxy-HbI and either the heme or residues at the interface as a function of the inverse of the variance, $\langle \delta r^2 \rangle^{-1}$, in the length of that contact. The data plotted in purple, which fall near the line with greater slope, correspond to hydrogen bonding between the heme and water molecules at the interface. The data plotted in green correspond to hydrogen bonding between interface water molecules and either lysine or arginine. Insets to (a) and (b) are schematic illustrations of the relation between fluctuations in the distance of a hydrogen bond and the rate of energy transfer between hydrogen-bonded residues, as quantified by the energy conductivity, G . Reprinted from (Leitner et al. 2019), Copyright (2019), American Chemical Society

Ishikura and Yamato 2006; Leitner and Yamato 2018), is multiplied by RT , and values of G are plotted in $(\text{kcal mol}^{-1})^2 \text{ps}^{-1}$.

Figure 3 is a plot of G vs. $\langle \delta r^2 \rangle^{-1}$ for polar contacts of HbI in the unliganded state. We define polar contacts as $X-H\cdots Y$, where X and Y are either N or O and the $H\cdots Y$ separation is no greater than 2.8 Å. Hydrogen bonds, a sub-class of polar contacts and in practice the large majority of them, are those with angles $XHY \geq 150^\circ$. For all contacts that exist for at least 99% of the trajectory, we calculate the average distance between the atoms forming the polar contact, $\langle r \rangle$, and the variance in the distance, $\langle \delta r^2 \rangle = \langle (r - \langle r \rangle)^2 \rangle$, and subsequently pair the variance with the respective energy conductivity, G , computed for the trajectory. We eliminate trajectories with small G and to reduce noise at small $\langle \delta r^2 \rangle^{-1}$ and only plot data with G exceeding a threshold of 50 $(\text{kcal mol}^{-1})^2 \text{ps}^{-1}$.

Polar contacts within the globules of unliganded HbI are plotted in Fig. 3(a) and between water and interface residues in Fig. 3(b), specifically for contacts between the interface water cluster and either the heme (purple) or some of the residues at the interface (green) that strongly couple to the water, which are side chains of lysine and arginine. In Fig. 3(a), the polar contacts exclude hydrogen bonds along α -helices, which follows the rule for energy transport along the main chain (Buchenberg et al. 2016). As found for myoglobin, the computational data for G across hydrogen bonds in each globule of HbI in the unliganded state fall along two different lines (Reid et al. 2018). Interestingly, comparing Fig. 3(a) and (b), we see that the data for contacts with water exhibit an energy conductivity that is comparable to or even larger than that found for residue pairs. Overall, since G is proportional to the energy transfer rate, w , the results plotted in Fig. 3 support the relation between energy transfer rate and equilibrium structural fluctuations, i.e., $w \propto \langle \delta r^2 \rangle^{-1}$. This establishes a relation between the energy conductivity, G (proportional to w), across polar contacts and equilibrium fluctuations in the length of the contact. The energy conductivity indeed reveals information about protein dynamics, not only structure, and the EEN for a protein in a functional state contains information both about the range of structures sampled by the protein in that state as well as the dynamics. We note that the local energy diffusivity, which we have also computed (Leitner et al. 2015), can be readily converted to a rate constant for energy transfer between residue pairs, which can in turn be compared with energy transfer rates obtained by molecular simulations and experiments. Energy conductivity is proportional to the energy diffusivity and hence the rate, the details of which we are currently evaluating.

Summary and future directions

An energy exchange network (EEN) embodies both structural and dynamical information about a protein in a functional

state. When there is a change of state, we have seen with the example of FixL, as in earlier studies of PDZ (Ishikura et al. 2015) and HbI (Gnanasekaran et al. 2011; Leitner 2016), that the Δ EEN map identifies residues important in this process, indicating networks involved in allosteric transitions. Structural biology alone cannot fully capture the network. While the network depends on the presence of contacts through which energy transport occurs, we have seen that the magnitude of the energy conductivity between non-bonded contacts depends sensitively on the dynamics of the contact. Equilibrium structural fluctuations influence the EEN for a particular functional state of a protein, as well as the range of structures of the protein in that state.

We have reviewed recent work on myoglobin and HbI indicating connections between energy conductivity, proportional to the rate of energy transfer, across non-bonded contacts interacting by hydrogen bonds and equilibrium fluctuations in the length of the contact. In an early computational study of HP36 (Buchenberg et al. 2016), the rate of energy transfer across a non-bonded contact was found to be proportional to the inverse of the variance in the contact length, both for polar contacts and van der Waals contacts. That work was carried out at low temperature to improve signal to noise. We have seen that the relation holds up well for polar contacts of myoglobin and HbI at 300 K. Nevertheless, we still do not have a complete picture of the scope of applicability of this scaling relation. For instance, for long-range ionic contacts, we have found that a diffusion picture is supported by computational results, which depends on the number of simultaneously interacting ions, but at shorter range, it is not clear whether the rate of energy transfer is proportional to the inverse of the variance in the length of the contact. It appears that simultaneous interactions among ions complicates such a relation at short range, which computational results indicate may not follow the same relation as we have seen for hydrogen bonds to date (Reid et al. 2018).

Future computational work will be needed to explore these trends in more detail, both for longer range interactions, as well as for short-range interactions, including van der Waals. The proportionality between the rate of energy transfer across a contact and the inverse in the variance of contact length has not yet been thoroughly investigated computationally for van der Waals contacts since the energy conductivity across van der Waals contacts is usually small compared to values across hydrogen bonds, and at 300 K, there is relatively large noise in the data. We are currently carrying out extensive simulations on HP36 at 300 K, and evaluating the energy conductivity across van der Waals contacts with CURP to more carefully examine the relation to equilibrium dynamics at this temperature.

Further experimental work in this area is still needed. In this context we mention important time-resolved Raman experiments carried out by Mizutani and coworkers (Fujii et al.

2011, 2014; Kondoh et al. 2016; Mizutani 2017; Yamashita et al. 2018). One recent study indicates that the rate of energy transfer from the heme to Trp68, tightly packed against each other by van der Waals contacts, is not influenced by loss of the covalent linkage between the heme and the protein via His93, a H93G mutant (Yamashita et al. 2018). Companion molecular dynamics simulations carried out on these systems suggest that the contact between the heme and Trp68 remains unchanged upon mutation to H93G (Yamashita et al. 2018). These results are consistent with the relation we have described between the rate of energy transfer across a non-bonded contact interacting by a short-range potential, including van der Waals interactions, and the equilibrium fluctuations of the contact, providing some support for the connection. Nevertheless, further support by experiments that probe contacts where the dynamics changes with mutation would be valuable. Such experiments could involve a variety of time-resolved vibrational techniques (Baumann et al. 2019; Hogle et al. 2018; Mizutani 2017; Nguyen et al. 2010; Rubtsov 2009), and we expect that new discoveries from these ongoing experimental studies will in turn stimulate the need to further explore relations between protein structure, dynamics, and energy transfer.

Acknowledgements Support from a JSPS Invitational Fellowship and NSF grant CHE-1854271 (DML) is gratefully acknowledged.

References

- Baumann T et al (2019) Observation of site-resolved vibrational energy transfer using a genetically encoded ultrafast heater. *Angew Chem* 58:2899–2903
- Buchenberg S, Leitner DM, Stock G (2016) Scaling rules for vibrational energy transport in proteins. *J Phys Chem Lett* 7:25–30
- Fujii N, Mizuno M, Mizutani Y (2011) Direct observation of vibrational energy flow in cytochrome c. *J Phys Chem B* 115:13057–13064
- Fujii N, Mizuno M, Ishikawa H, Mizutani Y (2014) Observing vibrational energy flow in a protein with the spatial resolution of a single amino acid residue. *J Phys Chem Lett* 5:3269–3273. <https://doi.org/10.1021/jz501882h>
- Gnanasekaran R, Agbo JK, Leitner DM (2011) Communication maps computed for homodimeric hemoglobin: computational study of water-mediated energy transport in proteins. *J Chem Phys* 135: 065103. <https://doi.org/10.1063/1.3623423>
- Hogle DG, Cunningham AR, Tucker MJ (2018) Equilibrium versus non-equilibrium peptide dynamics: insights into transient 2D IR spectroscopy. *J Phys Chem B* 122:8783–8795
- Ishikura T, Yamato T (2006) Energy transfer pathways relevant for long-range intramolecular signaling of photosensory protein revealed by microscopic energy conductivity analysis. *Chem Phys Lett* 432: 533–537
- Ishikura T, Iwata Y, Hatano T, Yamato T (2015) Energy exchange network of inter-residue interactions within a thermally fluctuating protein: a computational study. *J Comput Chem* 36:1709–1718. <https://doi.org/10.1002/jcc.23989>
- Kondoh M, Mizuno M, Mizutani Y (2016) Importance of atomic contacts in vibrational energy flow in proteins. *J Phys Chem Lett* 7:1950–1954

Leitner DM (2008) Energy flow in proteins. *Ann Rev Phys Chem* 59: 233–259

Leitner DM (2016) Water-mediated energy dynamics in a homodimeric hemoglobin. *J Phys Chem B* 120:4019–4027

Leitner DM, Straub JE (2010) Proteins: energy, heat and signal flow CRC press. Taylor & Francis Group, Boca Raton

Leitner DM, Yamato T (2018) Mapping energy transport networks in proteins. In: Parrill AL, Lipkowitz KB (eds) *Rev. Comp. Chem.*, vol 31. John Wiley & Sons, Inc., pp 63–114

Leitner DM, Buchenberg S, Brettel P, Stock G (2015) Vibrational energy flow in the villin headpiece subdomain: master equation simulations. *J Chem Phys* 142:075101

Leitner DM, Pandey HD, Reid KM (2019) Energy transport across interfaces in biomolecular systems. *J Phys Chem B* 123:9507–9524. <https://doi.org/10.1021/acs.jpcb.9b07086>

Mizutani Y (2017) Time-resolved resonance raman spectroscopy and application to studies on ultrafast protein dynamics. *Bull Chem Soc Jpn* 90:1344–1371

Nagy AM, Raicu V, Miller RJD (2005) Nonlinear optical studies of heme protein dynamics: implications for proteins as hybrid states of matter. *Biochim Biophys Acta* 1749:148–172

Nguyen PH, Hamm P, Stock G (2010) Nonequilibrium molecular dynamics simulation of photoinduced energy flow in peptides: theory meets experiment. In: Leitner DM, Straub JE (eds) *Proteins: energy, heat and signal flow*, CRC Press, Taylor & Francis Group, Boca Raton, pp 149–168

Ota K, Yamato T (2019) Energy exchange network model demonstrates protein allosteric transition: an application to an oxygen sensor protein. *J Phys Chem B* 123:768–775. <https://doi.org/10.1021/acs.jpcb.8b10489>

Reid KM, Yamato T, Leitner DM (2018) Scaling of rates of vibrational energy transfer in proteins with equilibrium dynamics and entropy. *J Phys Chem B* 122:9331–9339. <https://doi.org/10.1021/acs.jpcb.8b07552>

Reid KM, Yamato T, Leitner DM (2020) Variation of energy transfer rates across protein–water contacts with equilibrium structural fluctuations of a homodimeric hemoglobin. *J Phys Chem B* 124:1148–1159. <https://doi.org/10.1021/acs.jpcb.9b11413>

Rubtsov IV (2009) Relaxation-assisted two-dimensional infrared spectroscopy (RA 2DIR) method: accessing distances over 10 Å and measuring bond connectivity patterns. *Acc Chem Res* 42:1385–1394

Wright GSA et al (2018) Architecture of the complete oxygen-sensing FixL-FixJ two-component signal transduction system. *Sci Signal* 11:eaaq0825

Yamashita S, Mizuno M, Tran DP, Dokainish H, Kitao A, Mizutani Y (2018) Vibrational energy transfer from heme through atomic contacts in proteins. *J Phys Chem B* 122:5877–5884

Yamato T (2010) Energy flow pathways in photoreceptor proteins. In: Leitner DM, Straub JE (eds) *Proteins: energy, heat and signal flow*, CRC Press, Taylor and Francis Group, Boca Raton, pp 129–147

Publisher's note Springer Nature remains neutral with regard to jurisdictional claims in published maps and institutional affiliations.